

**Magnetic properties of the 3d transition metals in the amorphous ternary alloys:  $Gd_{0.2}(Fe_xCo_{1-x})_{0.8}$ ,  $Gd_{0.2}(Co_xNi_{1-x})_{0.8}$ , and  $Gd_{0.2}(Fe_xNi_{1-x})_{0.8}$**

R. C. Taylor and A. Gangulee

*IBM Thomas J. Watson Research Center, Yorktown Heights, New York 10598*

(Received 27 December 1979)

A systematic study was made of the magnetic properties of the amorphous alloys:  $Gd_{0.2}(Fe_xCo_{1-x})_{0.8}$ ,  $Gd_{0.2}(Co_xNi_{1-x})_{0.8}$ , and  $Gd_{0.2}(Fe_xNi_{1-x})_{0.8}$ . Results indicate that GdCo, GdNi, and GdCoNi alloys are collinear ferrimagnets involving electron transfer from Gd to the 3d elements. However, GdFe, GdFeNi, and GdFeCo alloys containing less than 30% Co are sperimagnetic due to antiferromagnetic interactions in the Fe subnetwork. Mean-field exchange energies are calculated and used to explain the results. A Slater-Pauling-type curve is constructed, and the dependence of properties on the average number of transition-metal 3d electrons is discussed.

## I. INTRODUCTION

We have recently reported on some of the magnetic properties of  $Gd_y(Fe_xCo_{1-x})_{1-y}$  (Ref. 1),  $Gd_y(Co_xNi_{1-x})_{1-y}$  (Refs. 2,3), and  $Gd_y(Fe_xNi_{1-x})_{1-y}$  (Ref. 4) amorphous thin films. The present study concentrates on ternary alloys with 20 at. % Gd and expands the data to a larger range of transition-metal concentrations. The purpose is to examine the effect of the number of transition-metal 3d electrons on magnetic properties and the temperature dependence of magnetization. Because of the technological importance of rare-earth transition-metal alloys, the ability to be able to predict such properties is highly desirable. There are important device implications in being able to match the temperature dependence of magnetization of two materials and at the same time be able to vary properties such as anisotropy and coercivity independently. On a more fundamental level, by using a constant concentration of a well understood rare earth, such as Gd (which is an S-state collinear ferromagnet), we hoped to be able to carefully study such mechanisms as charge transfer and to construct a Slater-Pauling-type curve for the Fe, Co, Ni series. This has been done frequently for the amorphous ferromagnetic transition-metal metalloid alloys<sup>5</sup> and occasionally for polycrystalline alloys such as YFeCo,<sup>6</sup> but not for amorphous ferrimagnetic materials. Our results have shown that many properties can be correlated with the d-electron concentration but that interpretation of a Slater-Pauling curve is difficult in materials with high Fe concentrations because of the appearance of sperimagnetism, that is, the random orientation of the moments in one or both subnetworks of an amorphous magnet with two magnetic subnetworks.

## II. EXPERIMENTAL

Films of the ternary alloys were prepared by coevaporation of the elements from three electron beam sources. The films were deposited on glass substrates to a nominal thickness of 5000 Å. Thickness was determined by Talysurf, composition by electron microprobe analysis to a relative accuracy of  $\pm 5\%$ , and the amorphous nature of the films was established by a glancing angle x-ray technique. The concentration of Gd in the alloys was between 17 and 22 at. %. Ranges for the transition metals were:  $Gd_{0.2}(Fe_xCo_{1-x})_{0.8}$ ,  $0.94 > x > 0.38$ ;  $Gd_{0.2}(Co_xNi_{1-x})_{0.8}$ ,  $0.83 > x > 0.29$ ;  $Gd_{0.2}(Fe_xNi_{1-x})_{0.8}$ ,  $0.80 > x > 0.19$ . The temperature dependence of magnetization for the films was measured from 4.2–295 K using a force balance magnetometer with fields up to 18 kOe. Reported saturation magnetizations were obtained by extrapolating to zero field. *MH* loops were obtained at 4.2 K and at room temperature by means of a vibrating sample magnetometer. Saturation and anisotropy fields could be obtained from these loops. In all calculations of transition-metal atomic moments, it was assumed that Gd was a collinear magnetic subnetwork with an atomic moment of  $7\mu_B$ .

## III. RESULTS

The temperature dependence of magnetization for three alloys in which the concentrations of the two transition metals are approximately equal is shown in Fig. 1. Compensation points, the temperature at which the magnetization in a ferrimagnet changes sign, exist at 140 K for  $Gd_{0.18}(Fe_{0.50}Ni_{0.50})_{0.82}$  and at

275 K for  $\text{Gd}_{0.18}(\text{Co}_{0.51}\text{Ni}_{0.49})_{0.82}$ . On the low-temperature side of the compensation point, the alloy magnetization is dominated by the magnetization of the Gd magnetic subnetwork, and on the high-temperature side by the transition-metal subnetwork. The magnetization of  $\text{Gd}_{0.18}(\text{Fe}_{0.49}\text{Co}_{0.51})_{0.82}$  is dominated by the magnetization of the transition-metal subnetwork down to 4.2 K. The solid lines in Fig. 1 are mean-field-theory fits to the data following a model described earlier.<sup>3</sup> Fitted variables were the exchange energies  $J_{M-M}$ ,  $J_{M-\text{Gd}}$  and, to a limited extent, the transition-metal spin  $S_M$ . ( $M$  refers to one of the 3d transition metals, Fe, Co, or Ni.) Both magnitude of  $4\pi M_s$  and the shape of the  $4\pi M_s$  vs  $T$  curves were optimized. The calculated exchange energies, along with those for the corresponding binary alloys, are given in Table I.<sup>7-9</sup> For the most part, experimental Curie temperatures cannot be obtained due to the low crystallization temperatures of the alloys, about 500 K. The lack of experimental  $T_C$  makes the calculated exchange energies subject to about a 20% error,<sup>3</sup> although spin values are much more accurate. Several compositions within each ternary series were analyzed and the exchange energies were found to fall within the 20% error, so that only an average, composition-independent value is given. In all cases, the following values were assumed for Gd spin, Gd exchange energy, and  $g$  factors:  $S_{\text{Gd}} = 3.5$ ,  $J_{\text{Gd-Gd}} = 2 \times 10^{-23}$  J,  $g_{\text{Fe}} = 2.15$ ,  $g_{\text{Co}} = 2.22$ ,  $g_{\text{Ni}} = 2.20$ , and  $g_{\text{Gd}} = 2.00$ .

The data for  $4\pi M_s$  versus composition at 4.2 K and at room temperature for all of the ternary alloys studied and three binary alloys are plotted in Fig. 2. Composition is given as the average number of transition-metal 3d electrons present in the alloy. The scatter appears to be due to the variation in Gd concentration of  $\pm 2$  at.%. With the exception of GdFeNi alloys, all experimental points with more than 20 at.% Gd lie above the 4.2-K line (more dominated by the Gd subnetwork magnetization) and all those with less than 20 at.% Gd lie below the line

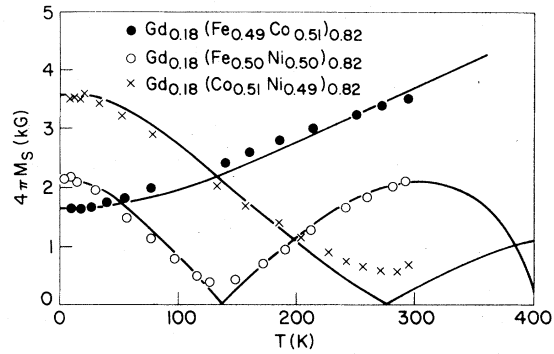


FIG. 1. Saturation magnetization as a function of temperature for  $\text{Gd}_{0.18}(\text{Fe}_{0.49}\text{Co}_{0.51})_{0.82}$ ,  $\text{Gd}_{0.18}(\text{Fe}_{0.5}\text{Ni}_{0.5})_{0.82}$ , and  $\text{Gd}_{0.18}(\text{Co}_{0.51}\text{Ni}_{0.49})_{0.82}$ . The solid lines are mean-field-theory fits to the data.

(more dominated by the transition-metal subnetwork magnetization). For the most part this is also true of the room-temperature line, although there is much less scatter in the room-temperature data. The value of  $4\pi M_s$  changes monotonically at 4.2° from a transition-metal-dominated value of 2000 G at 6 3d electrons (GdFe) to a rare-earth-dominated value of 9000 G at 8 3d electrons (GdNi) regardless of the transition metal involved. The room-temperature magnetization increases from a transition-metal dominated 2500 G at 6 3d electrons to 3500 G at about 6.4 3d electrons ( $\text{Fe}_{0.60}\text{Co}_{0.40}$  or  $\text{Fe}_{0.80}\text{Ni}_{0.20}$ ) and then decreases to zero at 7.6 3d electrons ( $\text{Fe}_{0.20}\text{Ni}_{0.80}$  or  $\text{Co}_{0.40}\text{Ni}_{0.60}$ ). The value of  $4\pi M_s$  then goes to a rare-earth dominant value of about 500 G at 7.7 3d electrons and then decreases to zero as the Curie temperature drops below room temperature. The range of composition for which a compensation point exists between 4.2 K and room temperature is from 6.7 to 7.6 3d electrons. Experimental compensation temperatures are plotted as a function of composition in Fig. 3.

TABLE I. Exchange energies (in joules) for  $\text{Gd}_{0.2}M_{0.8}$  and  $\text{Gd}_{0.2}(M_1)_{0.4}(M_2)_{0.4}$  alloys.

| Alloy              | $J_{\text{Fe-Fe}}$<br>( $10^{-21}$ ) | $J_{\text{Co-Co}}$<br>( $10^{-21}$ ) | $J_{\text{Ni-Ni}}$<br>( $10^{-21}$ ) | $J_{\text{Fe-Co}}$<br>( $10^{-21}$ ) | $J_{\text{Co-Ni}}$<br>( $10^{-21}$ ) | $J_{\text{Ni-Fe}}$<br>( $10^{-21}$ ) | $J_{\text{Fe-Gd}}$<br>( $10^{-22}$ ) | $J_{\text{Co-Gd}}$<br>( $10^{-22}$ ) | $J_{\text{Ni-Gd}}$<br>( $10^{-22}$ ) |
|--------------------|--------------------------------------|--------------------------------------|--------------------------------------|--------------------------------------|--------------------------------------|--------------------------------------|--------------------------------------|--------------------------------------|--------------------------------------|
| Gd-Fe <sup>a</sup> | 0.55                                 | ...                                  | ...                                  | ...                                  | ...                                  | ...                                  | -2.6                                 | ...                                  | ...                                  |
| Gd-Co <sup>b</sup> | ...                                  | 1.7                                  | ...                                  | ...                                  | ...                                  | ...                                  | ...                                  | -2.5                                 | ...                                  |
| Gd-Ni              | ...                                  | ...                                  | 0.8                                  | ...                                  | ...                                  | ...                                  | ...                                  | ...                                  | -0.5                                 |
| Gd-Fe-Co           | 0.5                                  | 2.2                                  | ...                                  | 1.6                                  | ...                                  | ...                                  | -2.1                                 | -2.3                                 | ...                                  |
| Gd-Co-Ni           | ...                                  | 2.9                                  | 1.0                                  | ...                                  | 1.1                                  | ...                                  | ...                                  | -1.8                                 | -1.3                                 |
| Gd-Ni-Fe           | 0.5                                  | ...                                  | 1.1                                  | ...                                  | ...                                  | 1.0                                  | -1.4                                 | ...                                  | -1.2                                 |

<sup>a</sup>From Ref. 7.

<sup>b</sup>From Refs. 8 and 9.

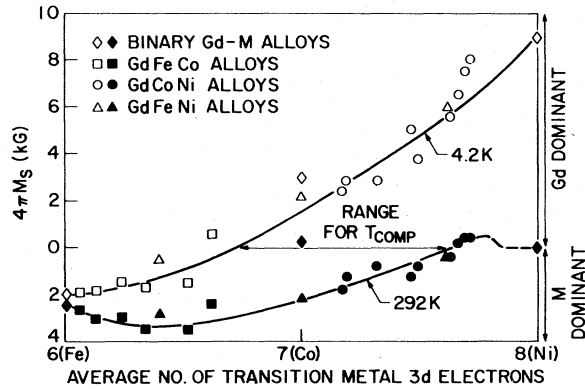


FIG. 2. Saturation magnetization vs composition (expressed as the average number of transition-metal  $3d$  electrons in the alloy) at 4.2 K and room temperature for GdFeCo, GdCoNi, and GdFeNi alloys.

It can be seen that the difference in  $4\pi M_s$  for a given composition between 4.2° and room-temperature values increases as the  $3d$ -electron concentration increases. This is shown in Fig. 4 where  $\Delta M$  is plotted against composition. The line in Fig. 4 is the difference between the two lines in Fig. 2. Again, with the exception of GdFeNi and GdCo alloys, films with more than 20 at. % Gd lie above the line and those with less than 20 at. % lie below the line. Apparently, parallel curves could be drawn for films with 15 at. % Gd, 25 at. % Gd, etc.

A clear illustration of the effect of  $3d$ -electron concentration on the temperature dependence of magnetization is given in Fig. 5 where  $4\pi M_s$  is plotted against temperature for four alloys. The alloys

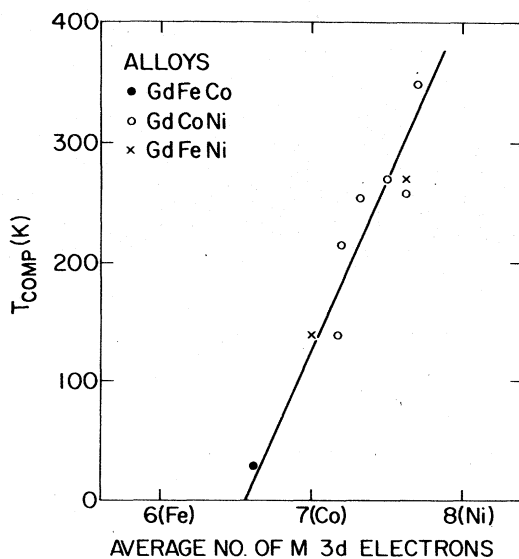


FIG. 3. Compensation temperature vs composition for GdFeCo, GdCoNi, and GdFeNi alloys.

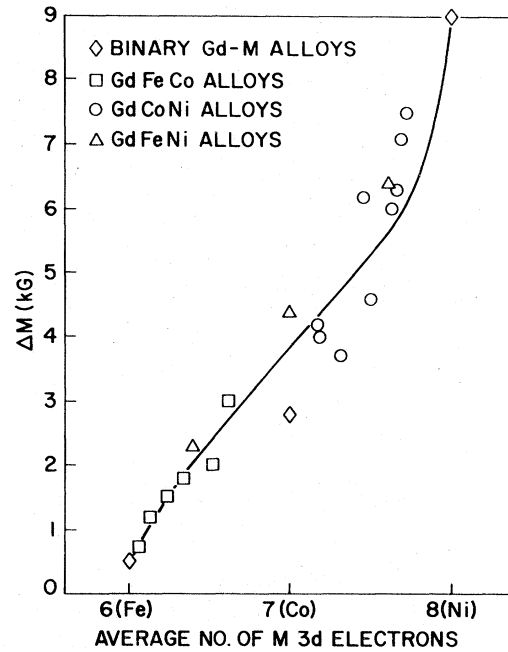


FIG. 4. Difference between  $4\pi M_s$  values at 4.2 K and at room temperature as a function of composition.

$Gd_{0.20}(Co_{0.38}Ni_{0.62})_{0.80}$  and  $Gd_{0.17}(Fe_{0.18}Ni_{0.82})_{0.83}$  both have the same average number of  $3d$  electrons per transition-metal atom, 7.63, and have virtually identical dependences of  $4\pi M_s$  on temperature. Similarly, the alloys  $Gd_{0.18}(Fe_{0.49}Co_{0.51})_{0.82}$  and  $Gd_{0.18}(Fe_{0.80}Ni_{0.20})_{0.82}$  have average  $3d$ -electron concentrations of 6.51 and 6.39, respectively. Although the moments are slightly different, the temperature dependence of the moments is again about the same. Thus, while absolute moments might be different due to the atomic moments of the constituents, especially at 4.2°, it seems that  $\Delta M/\Delta T$  is a function of

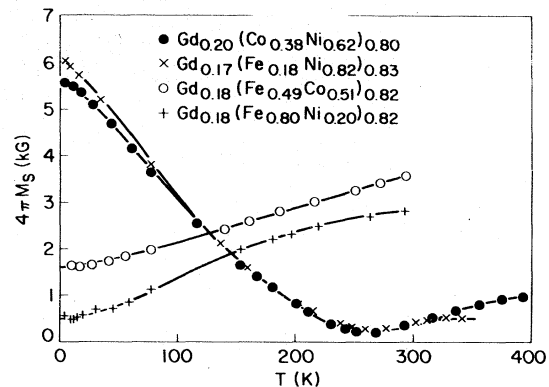


FIG. 5. Saturation magnetization vs temperature for the alloys  $Gd_{0.20}(Co_{0.38}Ni_{0.62})_{0.80}$ ,  $Gd_{0.17}(Fe_{0.18}Ni_{0.82})_{0.83}$ ,  $Gd_{0.18}(Fe_{0.49}Co_{0.51})_{0.82}$ , and  $Gd_{0.18}(Fe_{0.80}Ni_{0.20})_{0.82}$ .

the transition-metal 3d-electron concentration. Figure 5 shows that the FeNi alloys seem to be more Gd dominated at 4.2° than the other alloys. We have seen in *MH* loops taken at 4.2° that alloys high in Fe are difficult to saturate. High-field-susceptibility measurements at 4.2 K show that the volume susceptibility of  $\text{Gd}_{0.20}\text{Fe}_{0.80}$  is  $5.0 \times 10^{-3}$  and those of  $\text{Gd}_{0.18}(\text{Fe}_{0.49}\text{Co}_{0.51})_{0.82}$  and  $\text{Gd}_{0.18}(\text{Fe}_{0.50}\text{Ni}_{0.50})_{0.82}$  are  $3.9 \times 10^{-3}$  and  $2.3 \times 10^{-3}$ , respectively. The volume susceptibility of GdCo alloys is about  $0.9 \times 10^{-3}$  while those of  $\text{Gd}_{0.20}\text{Ni}_{0.80}$  and  $\text{Gd}_{0.21}(\text{Co}_{0.54}\text{Ni}_{0.46})_{0.79}$  are zero. All alloys saturate readily at room temperature.

Anisotropy constants have been determined at 4.2 K and at room temperature for all alloys. They all appear to have positive anisotropy (magnetically easy perpendicular axis) at 4.2 K, but only those with more than 50 at. % Fe (of *M* content) have positive anisotropy at room temperature. Thus, the anisotropy constant of  $\text{Gd}_{0.18}(\text{Fe}_{0.49}\text{Co}_{0.51})_{0.82}$  changes from  $3.1 \times 10^5$  ergs/cm<sup>3</sup> at 4.2° to  $-1.0 \times 10^5$  at room temperature. This is due to the differences in rate of change of magnetization with temperature of the various magnetic subnetworks, based on a pair-ordering model.<sup>1</sup> Room-temperature perpendicular anisotropies are given as a function of composition in Fig. 6.

The transition-metal atomic moments for all of the alloys were calculated from 4.2-K magnetization data by assuming a Gd moment of  $7\mu_B$  and using the

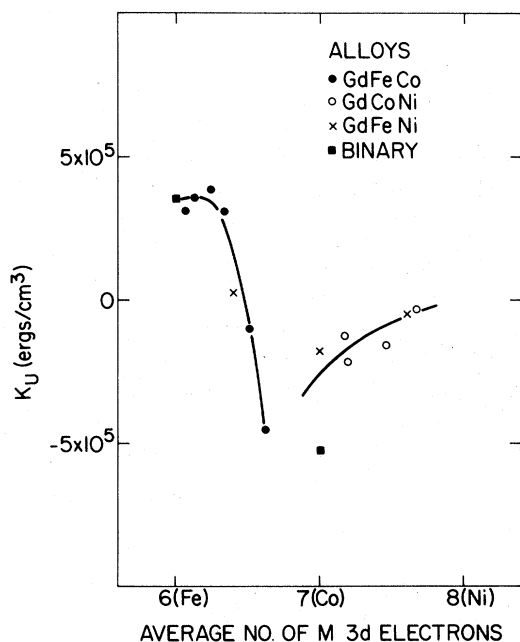


FIG. 6. Room-temperature perpendicular anisotropy constant vs composition for GdFeCo, GdCoNi, and GdFeNi alloys.

equation<sup>10</sup>

$$X_{\text{Gd}}(7\mu_B) + X_M(\mu_M) = (M_s/5585)(\bar{W}/\bar{\rho}) ,$$

where  $X_{\text{Gd}}$  and  $X_M$  are atomic fractions,  $\bar{W}$  is the average molecular weight,  $\bar{\rho}$  is the average density of the alloy, and  $\mu_M$  is the moment in Bohr magnetons of the transition-metal subnetwork. The resultant  $\mu_M$  as a function of 3d-electron concentration is plotted as a Slater-Pauling-type curve in Fig. 7. The lines represent calculated values for zero-, one-, two-, and three-electron transfer from Gd to the transition-metal subnetwork for FeCo and NiCo alloys. The zero transfer curves are those normally found for crystalline transition-metal alloys. FeNi-alloy lines may be drawn by connecting the end points. In calculating the Fe moment it was assumed that electrons transferred equally to the majority and minority *d* bands until the majority band was filled (0.4 electrons per Fe atom). Therefore, no increase is shown above the metallic Fe moment of  $2.22\mu_B$ . The calculated moments for the transition metals in the binaries are: Fe  $2.09\mu_B$ , Co  $1.45\mu_B$ , Ni  $0.31\mu_B$ . The data show that as Co is added to GdFe,  $\mu_M$  remains fairly constant to about  $\text{Fe}_{0.70}\text{Co}_{0.30}$  and then falls along the one-electron transfer line to GdCo. This indicates an increasing Fe moment with Co addition to a peak value of about  $2.3\mu_B$  after which both Fe and Co moments remain constant with further Co addition. As Ni is

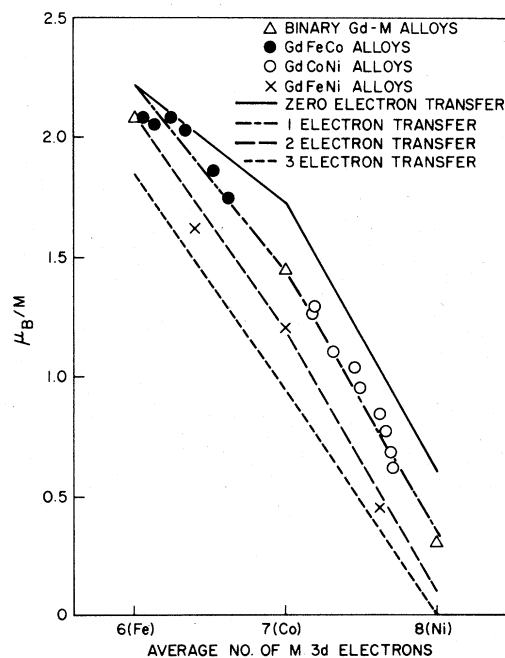


FIG. 7. Magnetic moment of the 3d-transition-metal subnetwork at 4.2 K as a function of composition for GdFeCo, GdCoNi, and GdFeNi alloys. The lines are calculated assuming electron transfer to the transition metals from Gd.

added to GdCo, the transition-metal subnetwork moment falls linearly along the one-electron-transfer line to pure GdNi. Both the Co and Ni values therefore remain constant at their binary values of  $1.45$  and  $0.31\mu_B$ . In the case of the GdFeNi alloys, the addition of Ni to GdFe does not increase the moment of Fe as did Co. Continued addition of Ni causes  $\mu_M$  to fall along the calculated two-electron-transfer line. Allowing for some scatter in the data, mean-field fitting shows that the Fe moment remains fairly constant while the Ni moment shows a slight decrease as its concentration increases.

A comparison between the behavior of the Gd alloys and that of transition-metal-metalloid alloys is shown in Fig. 8. The data of Durand<sup>11</sup> for  $(\text{NiFe})_{0.79}\text{P}_{0.13}\text{B}_{0.08}$  and of Mizoguchi *et al.*<sup>12</sup> for  $(\text{FeCo})_{0.80}\text{P}_{0.10}\text{B}_{0.10}$  and  $(\text{FeNi})_{0.80}\text{P}_{0.10}\text{B}_{0.10}$  have been used since their results most closely approximate our own. Our results for GdFeNi alloys correspond almost exactly with those of Durand, who explains his data by assuming that  $\mu_{\text{Fe}}$  remains constant at  $2.02\mu_B$  and that  $\mu_{\text{Ni}}$  increases from virtually zero at 100 at. % Ni to  $0.4\mu_B$  at 70 at. % Ni and then remains fairly constant as Ni content increases. The Ni atoms are assumed to be progressively polarized as Fe content increases in the same way that Pd is polarized in the crystalline PdFe system. Mizoguchi attributes his results to a rigid-band model with the spin-up band

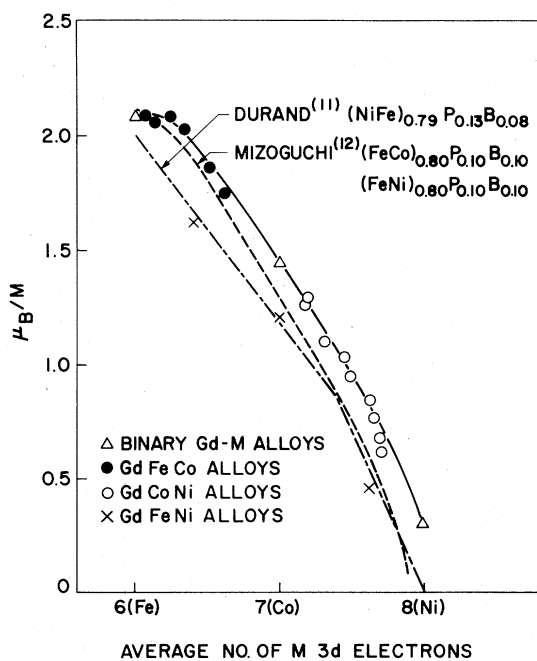


FIG. 8. A comparison of the change in transition-metal magnetic moment as a function of composition in Gd-transition-metal alloys and in transition-metal-metalloid alloys.

full and an increasing number of transferred electrons entering the spin-down band. Thus, there is no maximum in the FeCo data. The Fe maximum which we find is commonly seen with Co addition in a transition-metal-metalloid system, but not with Ni addition.<sup>5,13</sup>

#### IV. DISCUSSION

The combination of our results on Gd alloys and previous results on transition metals in combination with metalloids or nonmagnetic rare earths lead to the following conclusions:

(1) GdCo, GdNi, and GdCoNi are collinear ferromagnets in which each Gd atom transfers about 1 electron to the  $3d$  states of the transition metal.

(2) As indicated by its low-moment and high-field susceptibility at  $4.2^\circ$ , Fe in GdFe is partially antiferromagnetic or asperomagnetic (random ferromagnetism in the Fe subnetwork with the spins in random orientation around a preferential direction).

Several papers have appeared on amorphous alloys with one transition metal in combination with metalloids or elements such as Y which find that Co and Ni are ferromagnetic subnetworks but that the Fe subnetwork is partially antiferromagnetic, especially at high concentrations. Coey<sup>14</sup> has found that YCo and YNi are ferromagnets but that YFe has a random, noncollinear structure with a net moment (asperomagnetic). The Fe-Fe exchange in rare-earth-transition-metal alloys is not invariably ferromagnetic but is a sensitive function of atom separation. The exchange interaction distribution fluctuates about  $J = 0$  and is more likely to have either sign than is Co or Ni. Thus, even though the exchange interaction is much greater than local anisotropy, Fe remains asperomagnetic and complete alignment of the subnetwork cannot be attained even at very high fields.

Heiman and Kazama<sup>15,16</sup> have obtained similar results with alloys of Co and Fe with Y, La, Zr, and Lu. In YCo alloys there is a simple charge transfer with Y giving up 1.4 electrons to Co  $d$  states, and the Co moment is independent of rare-earth size. However, the Fe moment (and Fe-Fe exchange) is dependent on rare-earth size because of large exchange fluctuations and a small  $J_{\text{Fe-Fe}}$  as compared to a large  $J_{\text{Co-Co}}$  which is insensitive to structure fluctuations. Heiman claims that in the magnetic phase diagram the Fe exchange fluctuations span the region from ferromagnetism to spin-glass.

Additional evidence for Fe noncollinearity comes from Buschow *et al.*<sup>17</sup> and Durand.<sup>18</sup> Buschow found that alloys of Fe with Y, Th, or Zr had magnetizations which were strongly field dependent at 18 kOe and concluded that the alloys were random antiferromagnets. Charge transfer was also involved.

Durand in studies of amorphous FeBP claimed that Fe entered in both ferromagnetic and antiferromagnetic states. As Fe concentration decreased more of the Fe was polarized into the ferromagnetic state, as found in bcc crystalline Fe. This claim is reasonable in view of the facts that: (a) bcc crystalline Fe with eight nearest neighbors is ferromagnetic but fcc Fe with 12 nearest neighbors is antiferromagnetic, and (b) the number of nearest neighbors in these amorphous alloys is between 11 and 13 (Ref. 19); so that at large Fe concentrations the atomic structure begins to resemble that of a relaxed fcc Fe lattice. The unusually small magnitude of the self-exchange energy of Fe also seems to indicate the presence of significant amounts of the antiferromagnetic phase. The amount of antiferromagnetism is known to increase in amorphous alloys if one goes to transition metals with lower atomic number than Fe, such as in Mn or Cr metalloid films.<sup>12</sup>

With regard to ternary alloys containing Fe, our results lead to the additional conclusions:

(3) As Co is added to GdFe to form GdFeCo alloys, the antiferromagnetic Fe states are polarized to ferromagnetic states with all antiferromagnetic interactions disappearing by the time 30 at. % Co is added. The polarization is possible due to the high Fe-Co exchange interaction (see Table I) in conjunction with a high Co spin value and high Co-Co exchange interaction since the total magnetic interaction between two atoms,  $V_{ij}$ , is equal to  $-2J_{ij}\vec{S}_i \cdot \vec{S}_j$ .<sup>20</sup> Beyond 30 at. % Co, the GdFeCo alloys behave similarly to GdCoNi alloys, so that it is unlikely that additional charge transfer occurs. In addition the reduced numbers of Fe nearest neighbors of an Fe atom due to Co addition may also be expected to promote the ferromagnetic Fe phase. A similar situation occurs, for example, in polycrystalline CuMn films<sup>21</sup> and in amorphous GdMn films<sup>22</sup> where the Mn moment increases with decreasing Mn concentration.

(4) The addition of Ni to GdFe to form GdFeNi alloys apparently does not polarize the antiferromagnetic Fe states because of a low Fe-Ni exchange interaction along with a low Ni spin value and low  $J_{\text{Ni-Ni}}$ . Therefore, the moments of this alloy series remain lower than those containing Co over the entire composition range, the moment resulting from a combination of electron transfer and an asperomagnetic Fe subnetwork.

Calculations made by Jo<sup>23</sup> show the possibility of the existence of two magnetic states of Fe in NiFe crystalline alloys, with antiferromagnetic Fe states appearing when Fe exceeds 50 at. % in concentration. The deviation in the Slater-Pauling curve was explained by the presence of the two states.

Despite the asperomagnetic nature of Fe, the magnetization and temperature dependence of magnetization of the GdM alloys are predictable based on the average number of  $M$  3d electrons in the alloy. This is possibly due to the ferromagnetic alignment of the Fe with increasing temperature. This can be seen in Fig. 2 where less scatter exists in the room-temperature curve, in Fig. 5 where the 4.2 K difference in magnetization becomes smaller with increasing temperature, and in the fact that high-Fe samples saturate readily at room temperature although not at 4.2 K. The use of Mössbauer spectroscopy would help to clarify this point. Therefore, it is possible to match different materials with regard to their temperature dependence of magnetization while maintaining differences in properties such as anisotropy and coercivity.

#### ACKNOWLEDGMENTS

The authors wish to express their thanks to L. J. Buszko and H. R. Lilienthal for technical assistance and to R. C. O'Handley for helpful discussions.

<sup>1</sup>R. C. Taylor and A. Gangulee, *J. Appl. Phys.* **48**, 358 (1977).

<sup>2</sup>R. Hasegawa and R. C. Taylor, *J. Appl. Phys.* **46**, 3606 (1975).

<sup>3</sup>A. Gangulee and R. J. Kobliska, *J. Appl. Phys.* **49**, 4896 (1978).

<sup>4</sup>T. R. McGuire, R. C. Taylor, and R. J. Gambino, in *Magnetism and Magnetic Materials, 1976*, edited by J. J. Becker and G. H. Lander, AIP Conf. Proc. No. 34 (AIP, New York, 1976), p. 346.

<sup>5</sup>C. D. Graham, Jr., and T. Egami, *Ann. Rev. Mater. Sci.* **8**, 423 (1978).

<sup>6</sup>E. Burzo, *Solid State Commun.* **25**, 525 (1978).

<sup>7</sup>A. Gangulee and R. C. Taylor, *J. Appl. Phys.* **49**, 1762 (1978).

<sup>8</sup>R. C. Taylor and A. Gangulee, *J. Appl. Phys.* **47**, 4666 (1976).

<sup>9</sup>A. Gangulee and R. J. Kobliska, *J. Appl. Phys.* **49**, 4169 (1978).

<sup>10</sup>T. R. McGuire and P. J. Flanders, *Magnetism and Metallurgy I* (Academic, New York, 1969), p. 127.

<sup>11</sup>J. Durand, *Amorphous Magnetism II* (Plenum, New York, 1977), p. 305.

<sup>12</sup>T. Mizoguchi, T. Yamauchi, and H. Miyajima, *Amorphous Magnetism* (Plenum, New York, 1973), p. 325.

<sup>13</sup>R. C. O'Handley and D. S. Boudreaux, *Phys. Status Solidi A* **45**, 607 (1978).

<sup>14</sup>J. M. D. Coey, *J. Appl. Phys.* **49**, 1646 (1978).

<sup>15</sup>N. Heiman and N. Kazama, *Phys. Rev. B* **17**, 2215 (1978).

<sup>16</sup>N. Heiman and N. Kazama, *Phys. Rev. B* **19**, 1623 (1979).

- <sup>17</sup>K. H. J. Buschow, A. M. van Diepen, N. M. Beekmans, and J. W. M. Biesterbos, *Solid State Commun.* 28, 181 (1978).
- <sup>18</sup>J. Durand, *IEEE Trans. Magn.* 12, 945 (1976).
- <sup>19</sup>G. S. Cargill, III, *Solid State Physics* (Academic, New York, 1975), Vol. 30, p. 227.
- <sup>20</sup>J. S. Smart, *Magnetism III* (Academic, New York, 1963), p. 63.
- <sup>21</sup>R. W. Tustison and P. A. Beck, *Solid State Commun.* 20, 841 (1976).
- <sup>22</sup>T. R. McGuire and R. C. Taylor, *J. Appl. Phys.* 50, 1605 (1979).
- <sup>23</sup>T. Jo, *J. Phys. Soc. Jpn.* 40, 715 (1976).